CONF-860605--10

EFFECT OF COLD WORK ON TENSILE BEHAVIOR OF IRRADIATED TYPE 316 STAINLESS STEEL*

CONF-860605--10

DE86 008491

R. L. Klueh and P. J. Maziasz
Metals and Ceramics Division, Oak Ridge National Laboratory
Oak Ridge, TN 37831

ABSTRACT: The effect of various levels of cold work on the tensile behavior of type 316 stainless steel was investigated. Tensile specimens were irradiated in the Oak Ridge Research Reactor (ORR) at 250, 290, 450, and 500°C to produce a displacement damage of ~5 dpa and 40 at. ppm He. Irradiation at 250 and 290°C caused an increase in yield stress and ultimate tensile strength and a decrease in ductility relative to unaged and thermally aged controls. The changes were greatest for the 20%-cold-worked steel and lowest for the 50%-cold-worked steel. Irradiation at 450°C caused a slight relative decrease in strength for all cold-worked conditions. A large decrease was observed at 500°C, with the largest decrease occurring for the 50%-cold-worked specimen. No bubble, void, or precipitate formation was observed for specimens examined by transmission electron microscopy (TEM). The irradiation hardening was correlated with Frank-loop and "black-dot" loop damage. A strength decrease at 500°C was correlated with dislocation network recovery. Comparison of tensile and TEM results from ORR-irradiated steel with those from steels irradiated in the High Flux Isotope Reactor and the Experimental Breeder Reactor indicated consistent strength and microstructure changes.

KEY WORDS: stainless steel, cold work, neutron irradiation, microstructure, tensile properties, ductility, elevated temperature.

---

*Research sponsored by the Office of Fusion Energy, U.S. Department of Energy under Contract No. DE-AC05-840R21400 with Martin Marietta Energy Systems, Inc.

Introduction

Twenty-percent cold-worked type 316 stainless steel was chosen as the structural material for several core components of first-generation fast breeder reactors. It is also a candidate for the construction of the first-wall and blanket structure of fusion reactors. The choice of the cold-worked structure followed from the theoretical prediction [1] and experimental [2] observations that high dislocation densities should [1] and did [2] have an inhibiting effect on the void density, which should and did lead to a decrease in irradiation-produced swelling compared with a solution-annealed structure. Several studies have shown that cold working stainless steel leads to a reduction in swelling when the steel is irradiated between 0.3 and 0.5 T_m (T_m is the melting point) [3–6]. These investigations generally considered cold-work levels up to about 25 or 30%.

Although the reason for the choice of a 20%-cold-work level (as opposed to a higher or lower level) has not been widely discussed in the literature, the choice undoubtedly reflected a consideration of the properties of an unirradiated cold-worked steel as well as the effect of the cold-worked structure on swelling. Brager [6] did show that, for type 316 stainless steel, a 10%-cold-work level caused nearly as great a suppression of void formation as did 20% cold work. Above about 475°C, he found little difference in the swelling behavior of steels with 10 or 20% cold work; at 420°C (the lowest temperature investigated), there was very little difference between steel cold worked 20 and 30%.

Most irradiation studies on the effect of thermomechanical treatment (cold-work level and solution-anneal temperature) on type 316 stainless steel have examined the effect of irradiation on swelling. Little

information has appeared on the effect of preirradiation treatment on the irradiated tensile properties [7–9]. There is, however, considerable information available on the properties of solution-annealed (1 h at 1050°C) and 20%-cold-worked type 316 stainless steel irradiated in a fast reactor environment [8–12]. These irradiations in the Experimental Breeder Reactor (EBR-II) extend to 8.4×10^{26} neutrons/m^2 (>0.1 MeV). In addition to the irradiation in fast reactors, properties of solution-annealed and 20%-cold-worked type 316 stainless steel irradiated in the High Flux Isotope Reactor (HFIR), a mixed-spectrum reactor, have been reported [13–15].

In a fusion reactor, two types of irradiation effects are expected: displacement damage and large amounts of transmutation helium are produced by the high-energy neutrons. Therefore, it is of interest to determine the effect of both displacement damage and helium on properties. The effects of displacement damage alone can be studied by irradiation in a fast-spectrum fission reactor. The HFIR studies mentioned above were carried out as part of the fusion-reactor materials studies. HFIR has a mixed spectrum that contains both fast and thermal neutrons; thermal neutrons produce helium by a two-step reaction with ^{58}Ni in a nickel-containing alloy. Thus, irradiation of stainless steel in a mixed-spectrum reactor can produce both displacement damage and helium to approximately simulate fusion irradiations.

Helium can have pronounced effects on the mechanisms of void swelling, precipitation, and radiation-induced solute segregation in austenitic stainless steels under either ion or neutron irradiation [16–18]. Helium effects for fusion have been inferred from a comparison of the results from the EBR-II and HFIR irradiation of the same heat of

steel. However, neither of these reactor irradiations produces helium and displacement damage in type 316 stainless steel at the ratio to match fusion first-wall service (10—15 at. ppm He/dpa); HFIR produces far too much helium (20—70 at. ppm He/dpa) and EBR-II far too little (0.5—1 at. ppm He/dpa). The Oak Ridge Research Reactor (ORR) has a lower flux, but gives a better match to the helium/dpa generation ratio of a fusion first wall. This paper presents tensile and microstructural data obtained for type 316 stainless steel irradiated in the ORR.

Experimental Procedure

The type 316 stainless steel used in this study was taken from the Magnetic Fusion Energy (MFE) reference heat (X-15893); the chemical composition is given in Table 1.

Tensile specimens were machined from 0.76-mm-thick sheet. Specimens were obtained for sheet reduced by 20, 30, and 50%; prior to the final cold work, the steel was solution annealed 1 h at 1050°C. Material was also irradiated and tested that was aged for 10 h at 800°C after the 1 h at 1050°C anneal and prior to the 20%-cold work.

Sheet tensile specimens in this experiment were of the SS-1 type with a gage section 20.3-mm long by 1.52-mm wide by 0.76-mm thick. Specimens were irradiated in the E-7 position of the ORR in experiment ORR-MFE-2. These specimens were irradiated in holders that contained 22 sheet samples. The cylindrical holders were contained in a water-cooled aluminum block; each holder contained a central hole that contained an electric heater. Temperature was measured and controlled by two thermocouples located at the position of the center of the gage section in two unused sample positions located 180° apart.

Irradiation temperatures obtained in this experiment were approximately 250, 290, 450, and 500°C. The neutron fluence of ~6.8×10^{25} neutrons/m^2 (>0.1 MeV) produced ~5 dpa and the associated thermal neutron fluence of ~4.7×10^{25} neutrons/m^2 produced ~40 at. ppm He.

Tensile tests were made on unirradiated and irradiated specimens at the irradiation temperatures. Tests were conducted in a vacuum chamber on a 44-kN capacity Instron universal test machine at a strain rate of 4.2×10^{-5}/s.

Transmission electron microscopy (TEM) studies were made on the 20%-cold-worked material. Disks about 3 mm in diameter were electrodischarge machined from the shoulders of the tensile specimens that had been tensile tested. Previous work has established that the tensile testing does not disturb the as-irradiated microstructure in the shoulder region [19]. These samples were examined with the TEM techniques described previously [19,20]. The relatively high cobalt content of this alloy resulted in high levels of radioactivity after the ORR irradiation and made specimen handling difficult.

Results

The metallographic appearance of the cold-worked structure depended on the amount of cold work (Fig. 1); the grain structure was still clearly visible for the material deformed only 20%. When the solution anneal for 1 h at 1050°C was followed by the anneal for 10 h at 800°C, considerable precipitate formed on grain boundaries and within the matrix [Fig. 2(a)]. After this structure was cold worked 20%, the grain structure was easily seen by optical microscopy [Fig. 2(b)].

Tensile specimens were aged 4000 h (the approximate time of the irradiation experiment) at 300, 450, 500, and 650°C to determine the

effect of the thermal exposure on the properties (the higher temperature was used because these thermal aging results are to be used as controls for other experiments). The aged specimens were tested at the aging temperature and compared with the as-cold-worked material (Figs. 3–5).

Mechanical Properties

The 0.2% yield stress (YS) and ultimate tensile strength (UTS) of the unaged specimens showed the normal effects of cold work: The higher the amount of cold work, the higher the strength (Figs. 3 and 4). Thermal aging caused changes in strength, even at temperatures as low as 300°C, where a strength increase was observed over that of the unaged specimens. The strength advantage of the aged material was maintained up to about 500°C. At higher temperatures, however, the aged steel became weaker than the unaged steel, and the strength was significantly less after aging at 650°C for all cold-work levels. In fact, at 650°C, the weakest of the aged materials was the steel with 50% cold work.

The ductility of the unaged material inversely reflected the strength properties, with the strongest material (50% cold work) having the lowest ductility and the weakest having the highest ductility. The ductility of the unaged material appeared to reach a maximum between 500 and 600°C. Except at 650°C, the ductilities of the thermally aged specimens did not differ significantly from the unaged specimens. Upon aging, a large increase in ductility occurred at 650°C, which coincided with the large strength decrease. Just as the 50%-cold-worked steel showed the largest strength loss on aging at 650°C, it also showed the largest increase in ductility.

In Figs. 6 through 8, the tensile data for the irradiated specimens tested at 250 to 500°C are compared with the data for the thermally aged specimens. When irradiated, the YS and UTS of all three cold-worked levels increased over the corresponding unirradiated values at 250 and 290°C. The relative increase was inversely related to the level of prior cold work. Between 290 and 450°C there was a large decrease in the irradiation-produced strength; at 500°C, the strength of the irradiated steel fell below that of the unirradiated steel. Although the originally strongest 50%-cold-worked steel remained strongest after irradiation at 500°C, the irradiated strengths for the three cold-work levels appeared to be approaching a common value with increasing temperature.

The change in ductility of the irradiated cold-worked type 316 stainless steel does not directly reflect the increase in strength (Fig. 8). Both uniform and total elongations of the irradiated steels increased between 290 and 450°C, but they decreased between 450 and 500°C, even though the strength decreased. The steel with 20 and 30% cold work showed a large elongation increase between 290 and 450°C, whereas the 50%-cold-worked steel showed a much smaller increase. After irradiation at 500°C, the total elongation of the 50%-cold-worked steel was actually less than the value at 250°C. At all temperatures, the ductility reduction of the three steels maintained the inverse relationship with cold-work level that was true for the unirradiated material. However, in all cases the ductility of the irradiated steel was similar to that of the thermally aged steel.

For the three cold-work levels discussed above, the cold deformation followed a 1-h solution anneal at 1050°C. In Figs. 9 through 11

the strength and ductility of the type 316 stainless steel cold-worked 20% after the 1050°C solution anneal are compared with the steel cold-worked 20% following a 1050°C anneal plus a 10-h age at 800°C. Both before and after irradiation, there was very little difference in strength for these two steels. The uniform and total elongation values of the steel given the 800°C anneal did not increase between 290 and 450°C nearly as much as did the values for the other steel. This was true for both irradiated and unirradiated (aged and unaged) steels. However, the irradiated ductility values for both steels approached that for the unirradiated steels at 450 and 500°C.

Selected fracture surfaces were examined by scanning electron microscopy. All specimens displayed typical ductile shear-type failures. There was no indication of intergranular fracture at any irradiation or aging temperature on any material condition.

Transmission Electron Microscopy

The TEM studies on the irradiated 20%-cold-worked steel did not reveal any bubbles or voids in the microstructure of the steel irradiated in ORR to 5 dpa at temperatures from 250 to 500°C. There was also no evidence of precipitation for any of these irradiation conditions, although there was an effect of the irradiation on the dislocation structure.

After irradiation, the overall dislocation concentration was high and quite temperature independent from 250 to 450°C, but, by comparison, appeared much less concentrated at 500°C (Fig. 12). Frank loops (assumed to be interstitial) were a significant portion of the overall dislocation microstructure at all temperatures. The loop component at the various

temperatures is shown in Fig. 13 for one set of (111) planes [hence one-fourth of a total isotropic population of loops on (111) planes] imaged in dark field via <111> satellite streaks around g_{200} matrix reflections. A high concentration of loops ranging from 8 to 25 nm in diameter was observed from 250 to 450°C. Fewer, much larger (17 to 100 nm diameter) loops were observed at 500°C. The dislocation structures at 250 to 450°C appeared similar to or denser than the network normally found in the as-cold-worked material [18], but the dislocation structure at 500°C was somewhat recovered. Finally, a high concentration of "black dots" (<5 nm in diameter) can be seen in Fig. 12(a-c). These features, seen at 250 to 450°C when these samples were imaged in a weak-beam dark-field condition (g_{200}, +g/3g), may also be small loops. "Black dots" were not present after irradiation at 500°C.

Selected TEM specimens of the unaged and aged control specimens of the 20- and 50%-cold-worked specimens were examined to determine if the source of hardening during aging at 300 and 450°C could be detected. There was no indication of precipitation during aging nor any indication of a change in the dislocation structure that could be the cause of the hardening. The hardening must be associated with a solute-dislocation-locking mechanism (probably due to carbon).

Discussion

It is of interest to compare the results of these studies with irradiation effects observed after irradiation in HFIR, where much more helium is generated, and irradiation in EBR-II, where very little helium is generated. The comparison will be restricted to 20%-cold-worked material, as very few data are available for other cold-work levels.

Because most irradiation studies on 20%-cold-worked type 316 stainless steel have been conducted in conjunction with the fast-breeder program and have generally used EBR-II, few irradiations have been below about 370°C (limited by the EBR-II reactor coolant inlet temperature). Fish et al. [11,12] tested 20%-cold-worked type 316 stainless steel irradiated in EBR-II at temperatures between 371 and 816°C. They found an increase in both YS and UTS for material irradiated and tested below about 483°C, and only a slight amount of hardening was observed at 483°C. They reported softening of cold-worked material for irradiation and testing at 538°C and higher. This observation is similar to observations in the present tests on 20%-cold-worked type 316 stainless steel, where softening was observed at 500°C but not at 450°C. A similar observation was made for the steel with 30% cold work; however, the steel with 50% cold work softened at 450°C.

Tensile specimens of the 20%-cold-worked reference heat have been irradiated in HFIR, and where the irradiation and test temperatures were similar to those of the present experiment, similar tensile results were observed [15]. For tensile tests at 300°C of specimens irradiated at 284°C, the steel hardened to a saturation level. The strengths obtained in that experiment were similar to those obtained in this experiment for the 20%-cold-worked steel irradiated and tested at 290°C. This similarity occurred despite the fact that the HFIR-irradiated steel was irradiated up to 27 dpa and contained 1600 at. ppm He and confirms the saturation of strengthening at relatively low fluence levels.

The high dislocation density of a cold-worked structure retards void swelling because the dislocations act as sinks for irradiation-produced defects and traps for transmutation-product helium. Although

the higher dislocation density of the 50%-cold-worked structure would be expected to provide the highest irradiation resistance, the present results provide reasons for use of a lower cold-work level. Below ~550°C, the ductility of the 50%-cold-worked steel was lower than for the steel rolled 20 and 30% in the as-cold-worked, aged, and irradiated conditions. There is much less difference between the steels with 20- and 30%-cold work, especially after irradiation. It is also evident from the aging results that for temperatures above about 600°C, all of the cold-work levels rapidly lose strength as recrystallization occurs. At 650°C, the 50%-cold-worked steel is the weakest. Therefore, although the 50%-cold-work level would be expected to offer greater irradiation resistance at temperatures to ~550°C, the lower ductility for the higher cold-worked material may offset that advantage.

There have been extensive microstructural studies of 20%-cold-worked type 316 stainless steel irradiated in HFIR [18,20,23,24] and EBR-II [6,18,25], and these can be compared with the TEM studies on the ORR-irradiated material. Key features of the present results and the literature data are summarized in Figs. 14 and 15.

Bloom et al. [21] irradiated solution-annealed type 304 stainless steel in the ORR to fluences producing less than 0.5 dpa and less than about 5 at. ppm He at temperatures of 93 to 454°C. At 93°C, they observed a high density of fine "black-dot" structures, believed to be loops. With only small changes in size and density, this structure persisted at 177 and 300°C. At 371°C, the "black-dot" density decreased by several orders of magnitude; it disappeared at 398°C. Larger loops, precipitates, and small helium bubbles began to appear at 454°C.

Figures 14 and 15 define the temperature limits of these observations. Brager and Garner [22] also observed Frank loops, networks, and "small defect clusters" (<3 nm in diameter) in solution-annealed and cold-worked high-purity 316 austenitic stainless steel (P7) irradiated in ORR to 3 dpa at 350°C. They found voids and bubbles in P7 after irradiation to 4 dpa (33 at. ppm He) at 550°C, which is qualitatively consistent with the present results in that a fairly constant, low-temperature microstructure is observed over a range of temperatures before a transition occurs to a microstructure characteristic of higher temperatures. The transition (judging from loop and "black-dot" structures) occurs about 100 to 150°C higher for cold-worked 316 than for the solution-annealed 304 of Bloom et al.

The microstructural results on cold-worked 316 (reference heat) irradiated in ORR are consistent with microstructural data on several heats of steel [304, DO-heat and N-lot 316, and Path A Prime Candidate Alloy (PCA)] irradiated in HFIR in several microstructural conditions [19,20,23,24,26,28] (Figs. 14 and 15). No voids, bubbles, or irradiation-induced or -enhanced precipitates were observed after HFIR irradiation at 55 to 300°C, for fluences producing up to approximately 11 dpa. Regardless of material or pretreatment, the HFIR microstructures consisted of similar-sized Frank loops (~10—30 nm in diameter) and a high concentration of the "black-dot" defects (~3—5 nm in diameter) (Fig. 14). However, dislocation network concentration varied widely and depended strongly on pretreatment. Bubbles were found after HFIR irradiation at 400°C for some of the PCA pretreatments and for cold-worked 316 (N-lot). The very fine "black dots" were not observed when these materials contained bubbles [27]. These "black dots" were also absent when voids

appeared in cold-worked 316 (DO-heat) irradiated in HFIR at 325 to 350°C to 8.4 dpa. Again, this transition from characteristic lower temperature to higher temperature microstructure occurred at about 300 to 350°C in HFIR (Fig. 14), 100 to 150°C lower than for cold-worked 316 (reference heat) irradiated in ORR.

Fast-breeder reactor data do not extend below 300 to 350°C. However, the limited data are also mapped with temperatures in Figs. 14 and 15. Voids were not observed by Bramman et al. [28] in type 316 stainless steel irradiated below 350°C to 30 to 40 dpa in the Dounreay Fast Reactor. Voids were also not observed by Bloom and Stiegler [25] for cold-worked 316 (DO-heat) irradiated in EBR-II at 450°C to 10 dpa or at 510°C to 6.4 dpa. Maziasz [18] found no voids or fine bubbles in the same material irradiated in EBR-II to 8.4 dpa at 500°C, but found both voids and bubbles after 36 dpa at 525°C. Brager [26], however, observed voids in another heat of cold-worked 316 after EBR-II irradiation to 12.2 dpa at 420 and 475°C (Fig. 15). The early stages of void formation for type 316 stainless steel in EBR-II are extremely variable from heat to heat of steel. Within this scatter, however, the ORR results are consistent with EBR-II results (Fig. 15); it is not clear whether or not voids should be expected after only 5 dpa in the ORR at 450 to 500°C. Higher fluence data will be required before confident statements about retardation (or acceleration) of void or bubble formation in ORR can be made. Comparison with the HFIR data shows that bubble swelling at 500°C is retarded in ORR.

Summary and Conclusions

The effect of cold-work level on the tensile behavior of irradiated type 316 stainless steel was investigated. After irradiation in ORR at 250, 290, 450, and 500°C to ~5 dpa and 40 at. ppm He, tensile specimens with 20-, 30-, and 50%-cold work levels were tested at the irradiation temperatures. The results indicate that the use of a 20- to 30%-cold-worked steel has mechanical-property advantages over a steel cold worked to 50%, even though the latter may have the best swelling resistance. Although the steels with 20- and 30%-cold work are hardened relatively more at 250 and 290°C than steel with 50%-cold work, the ductility of the 20- and 30%-cold-worked steels remains significantly better than for the steel with 50%-cold work. For tests at 500°C where radiation-enhanced softening occurs, the properties for all three cold-work levels begin to approach a common value.

Transmission electron microscopy observations on the 20%-cold-worked steels were compared with results from EBR-II and HFIR. In EBR-II, little helium is produced relative to ORR; in HFIR, a much higher He/dpa ratio results than in ORR. No noticeable difference in microstructural evolution occurred for the samples irradiated in ORR and in the other two reactors.

Acknowledgments

We wish to thank the following people who helped in the completion of this work: L. T. Gibson and N. H. Rouse did the tensile tests; N. H. Rouse prepared the TEM specimens; F. W. Wiffen and N. H. Packan reviewed the manuscript; and Frances Scarboro prepared the manuscript.

REFERENCES

[1] Bullough, R., Eyre, B. L., and Perrin, J. S., Nucl. Appl. Technol., Vol. 9, 1970, pp. 346–355.

[2] Farrell, K. and Houston, J., J. Nucl. Mater., Vol. 35, 1970, pp. 352–355.

[3] Bramman, J. I. et al., Voids Formed by Irradiation of Reactor Materials, British Nuclear Energy Society, London, 1971, pp. 27–33.

[4] Cawthorne, C. et al., Ibid., pp. 35–43.

[5] Stiegler, J. O. and Bloom E. E., J. Nucl. Mater., Vol. 41, 1971, pp. 341–344.

[6] Brager, H. R., J. Nucl. Mater., Vol. 57, 1975, pp. 103–118.

[7] Kawasaki, S., Fukaya, K., and Nagasaki, R., Nippon Genshreryoko Gakkaishi, Vol. 14, 1972, pp. 283–289.

[8] Fahr, D., Bloom, E. E., and Stiegler, J. O., Irradiation Embrittlement and Creep of Fuel Cladding and Core Components, British Nuclear Energy Society, London, 1973, pp. 167–177.

[9] Garr, K. R., Pard, A. G., and Kramer, D., Properties of Reactor Structural Alloys after Neutron and Particle Irradiation, ASTM STP-570, Baroch, C. J., ed., American Society for Testing and Materials, Philadelphia, 1975, pp. 143–155.

[10] Garr, K. R. and Pard, A. G., Irradiation Effects on the Microstructure and Properties of Metals, ASTM STP-611, F. R. Shrober, ed., American Society for Testing and Materials, Philadelphia, 1976, pp. 79–90.

[11] Fish, R. L. and Waltrous, J. D., Ibid., pp. 91–100.

[12] Fish, R. L., Cannon, N. S., and Wire, G. L., Effects of Radiation on Structural Materials, ASTM STP-683, J. A. Sprague and K. Kramer, eds., American Society for Testing and Materials, Philadelphia, 1979, pp. 450–465.

[13] Bloom, E. E. and Wiffen, F. W., J. Nucl. Mater., Vol. 86, 1979, pp. 171–184.

[14] Grossbeck, M. L. and Maziasz, P. J., J. Nucl. Mater., Vol. 86, 1979, pp. 883–887.

[15] Klueh, R. L. and Grossbeck, M. L., Effects of Irradiation on Materials: Twelfth International Symposium, ASTM STP-870, F. A. Garner and J. S. Perrin, eds., American Society for Testing and Materials, Philadelphia, 1985, pp. 768–782.

[16] Odette, G. R., Maziasz, P. J., and Spitznagel, J. A., J. Nucl. Mater., Vols. 103&104, 1981, pp. 1289–1304.

[17] Lee, E. H., Rowcliffe, A. F., and Mansur, L. K., Ibid., pp. 1475–1480.

[18] Maziasz, P. J., J. Nucl. Mater., Vols. 108&109, 1982, pp. 359–384.

[19] Maziasz, P. J., Horak, J. A., and Cox, B. L., Phase Stability During Irradiation, J. R. Holland, L. K. Mansur, and D. I. Potter, eds., The Metallurgical Society of AIME, Warrendale, PA, 1981, pp. 271–292.

[20] Maziasz, P. J. and Grossbeck, M. L., J. Nucl. Mater., Vol. 104, 1982, pp. 987–992.

[21] Bloom, E. E., Martin, W. R., Stiegler, J. O., and Weir, J. R., J. Nucl. Mater., Vol. 22, 1967, pp. 68–76.

[22] Brager, H. R. and Garner, F. A., Effects of Irradiation on Materials, ASTM STP-782, H. R. Brager and J. S. Perrin, eds., American Society for Testing and Materials, Philadelphia, 1985, pp. 152–165.

[23] Wiffen, F. W. and Maziasz, P. J., J. Nucl. Mater., Vols. 103&104, 1981, pp. 821–826.

[24] Maziasz, P. J., Trans. Am. Nucl. Soc., Vol. 39, 1981, pp. 433–485.

[25] Bloom, E. E. and Stiegler, J. O., Effects of Radiation on Substructure and Mechanical Properties of Metals and Alloys, ASTM STP-529, J. Moteff, ed., American Society for Testing and Materials, Philadelphia, 1973, pp. 360–387.

[26] Maziasz, P. J. and Braski, D. N., J. Nucl. Mater., Vols. 122&123, 1984, pp. 305–310.

[27] Maziasz, P. J. and Braski, D. N., Ibid., pp. 311–316.

[28] Bramman, J. I. et al., Radiation Effects in Breeder Reactor Structural Materials, M. L. Bleiberg and J. W. Bennett, eds., The Metallurgical Society of AIME, Warrendale, PA, 1977, pp. 479–508.

TABLE 1—Chemical composition of type 316 stainless steel MFE reference heat X-15893

Element	Percent by Weight	Element	Percent by Weight
Cr	17.28	Nb	<0.05
Mn	1.70	Ta	<0.05
Ni	12.44	Ti	<0.05
Mo	2.10	B	0.0004
Co	0.3	C	0.061
Cu	0.3	S	0.018
Si	0.67	P	0.037

LIST OF FIGURES

Fig. 12. Dislocation microstructures of CW 316 (reference heat) irradiated in ORR to 5 dpa (38.7 at. ppm He) at (a) 250°C, (b) 290°C, (c) 450°C, and (d) 500°C. All are imaged using g_{200} with $s > 0$. Note the more relaxed structure at 500°C (d).

Fig. 13. Larger Frank loop component of the dislocation microstructure of CW 316 (reference heat) irradiated in ORR to 5 dpa (38.7 at. ppm He) at (a) 250°C, (b) 290°C, (c) 450°C, and (d) 500°C. All are imaged in dark field using <111> satellite streaks around g_{200} reflections. Note the large increase in size and decreased density of loops at 500°C, compared with the three lower temperatures.

Fig. 14. Temperature boundaries between the various components of the dislocation microstructure observed in austenitic stainless steels irradiated to fluences producing 12 dpa or lower.

Fig. 15. Observations at fluences producing 12 dpa or lower that define the lower temperature limit for cavity formation in austenitic stainless steel.

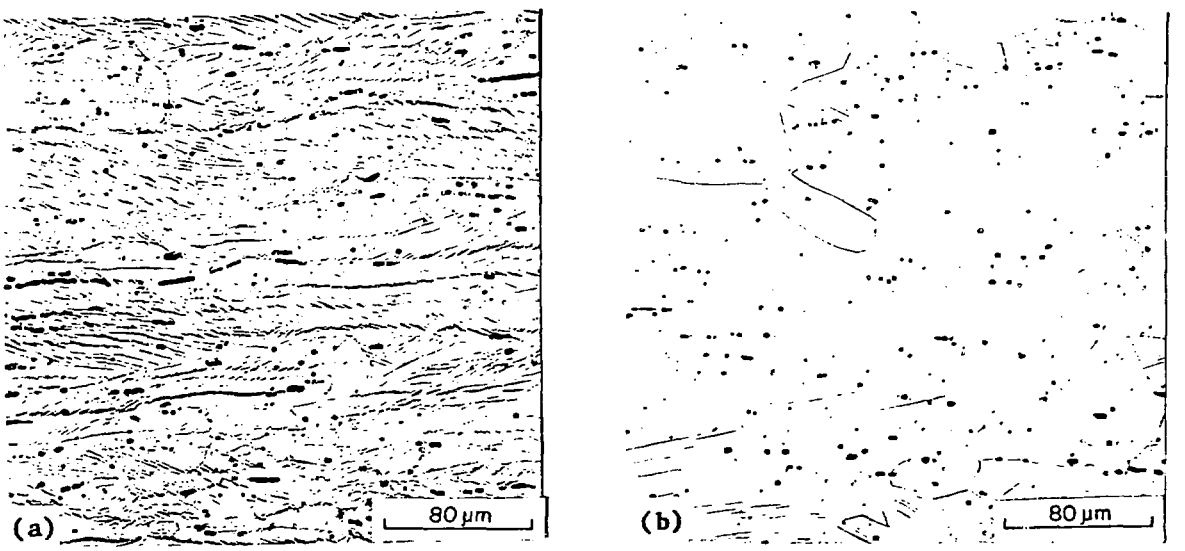

Fig. 1. Microstructure of type 316 stainless steel cold worked (a) 20% and (b) 50%.

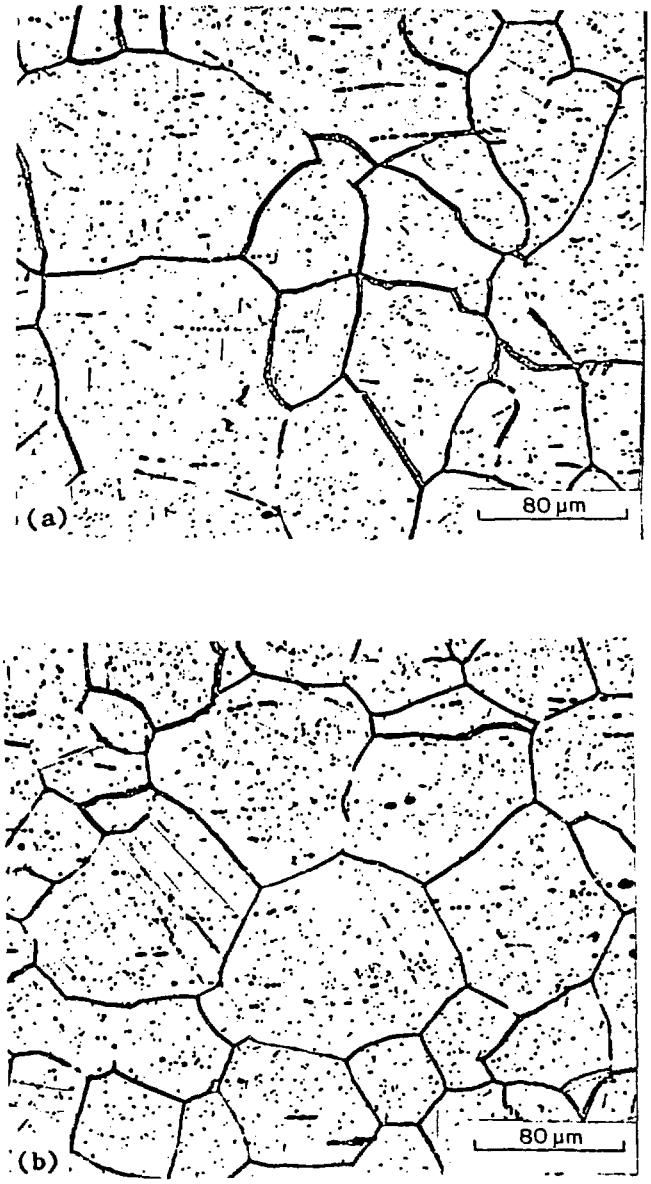

Fig. 2. Microstructure of type 316 stainless steel (a) solution annealed 1 h at 1050°C and then further annealed 10 h at 800°C, and (b) this steel after rolling 20%.

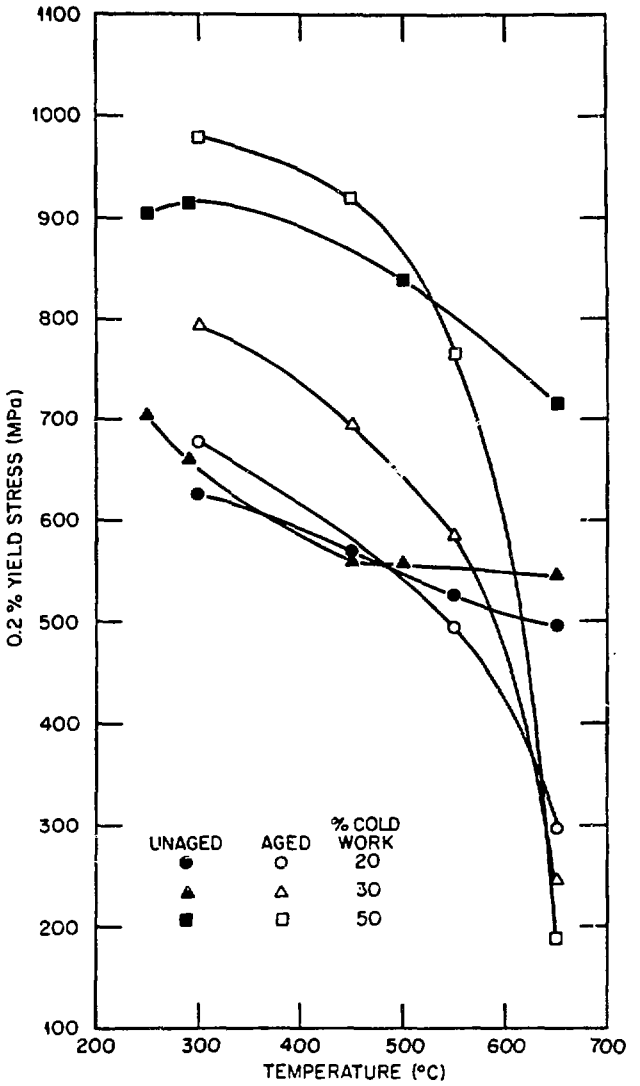

Fig. 3. The 0.2% yield stress of cold-worked and cold-worked and thermally aged type 316 stainless steel. Specimens were aged 4000 h at the same temperature used for the tests.

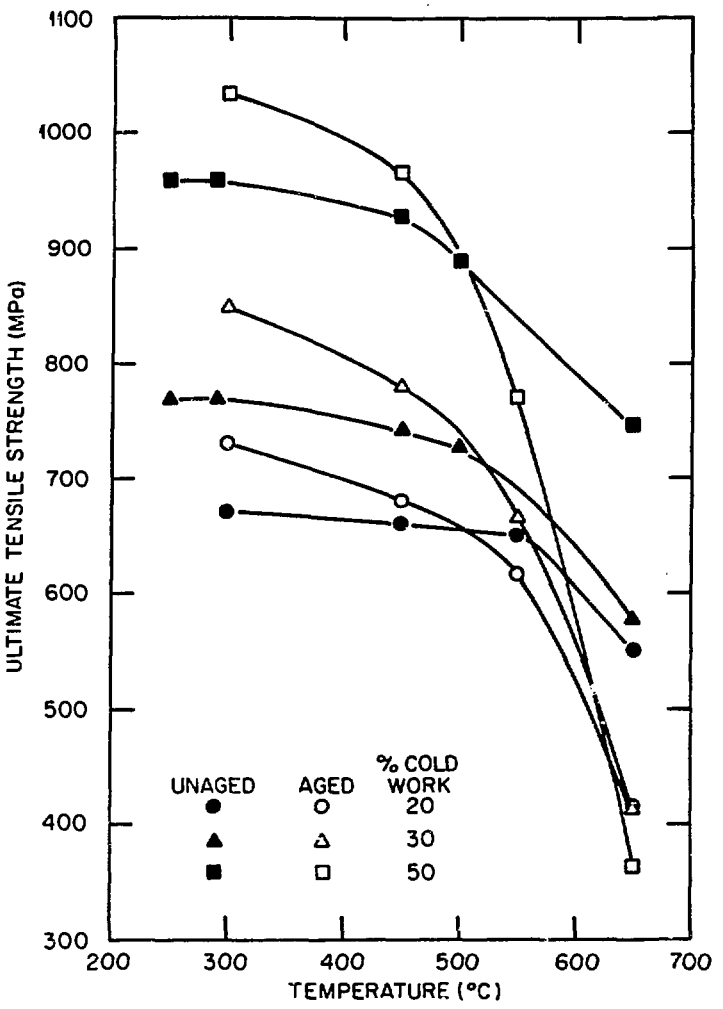

Fig. 4. The ultimate tensile strength of cold-worked and cold-worked and thermally aged type 316 stainless steel. Specimens were aged 4000 h at the same temperature used for the tests.

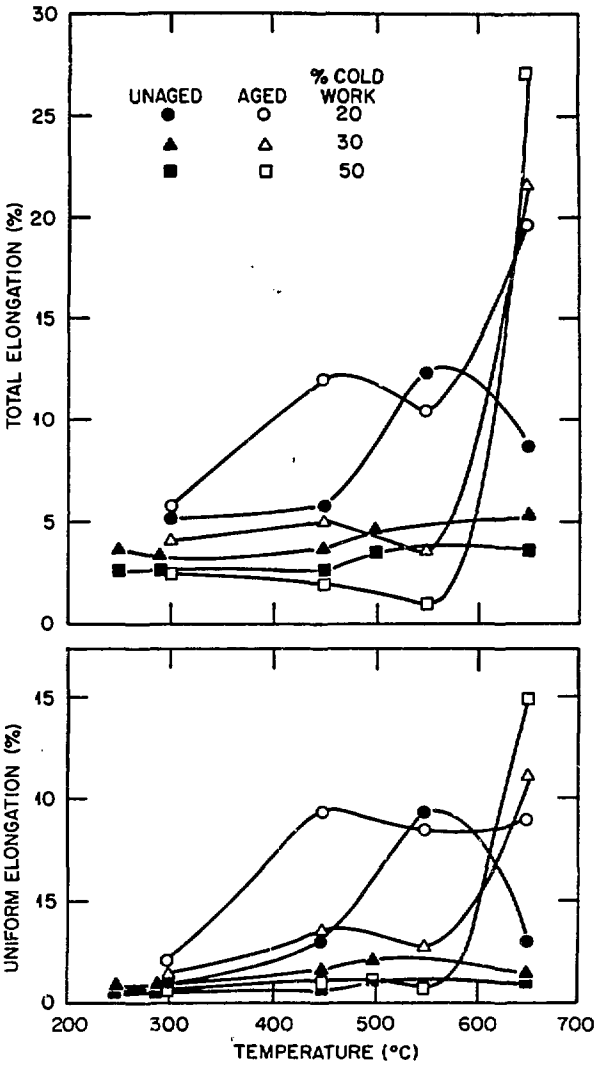

Fig. 5. The uniform and total elongation of cold-worked and cold-worked and thermally aged type 316 stainless steel. Specimens were aged 4000 h at the same temperature used for the tests.

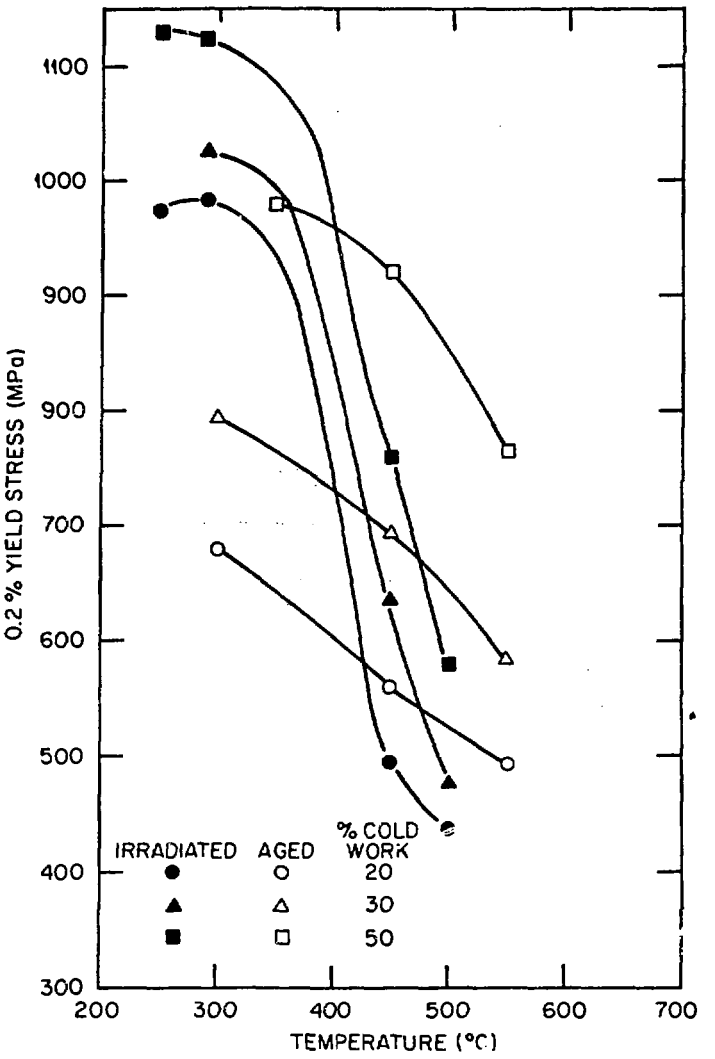

Fig. 6. The 0.2% yield stress of the thermally aged and the irradiated cold-worked type 316 stainless steel. Tests were at the aging and irradiation temperatures.

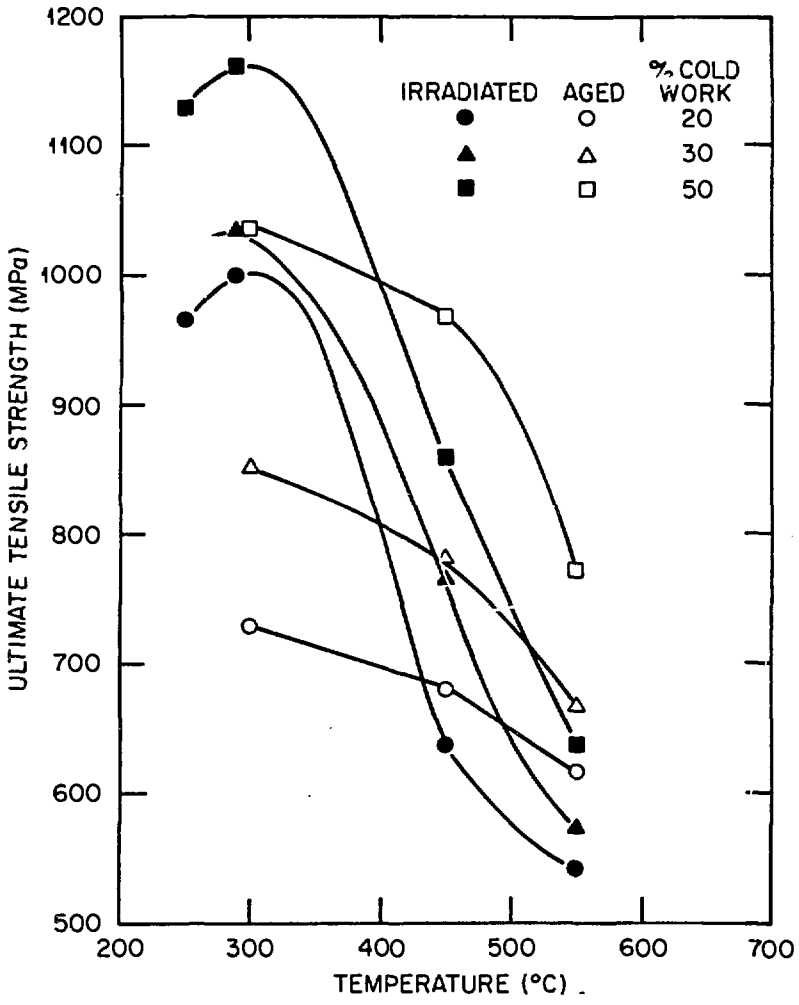

Fig. 7. The ultimate tensile strength of the thermally aged and the irradiated type 316 stainless steel. Tests were at the aging and irradiation temperatures.

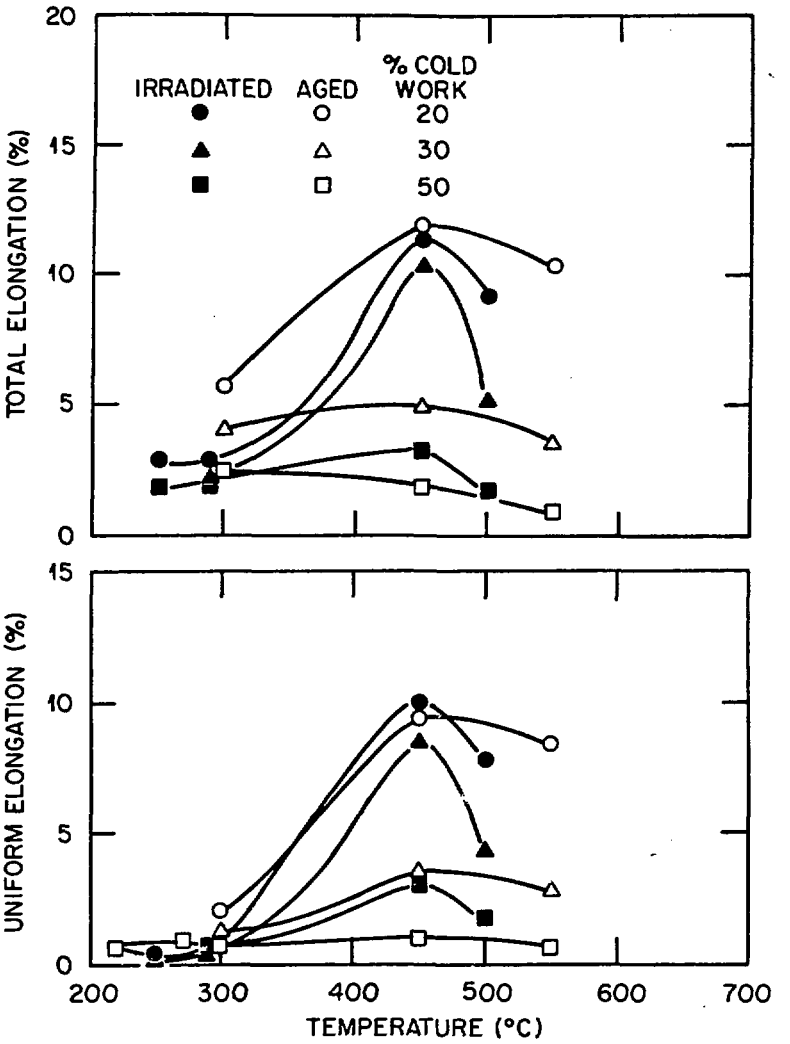

Fig. 8. The uniform and total elongations of the thermally aged and irradiated type 316 stainless steel. Tests were at the aging and irradiation temperatures.

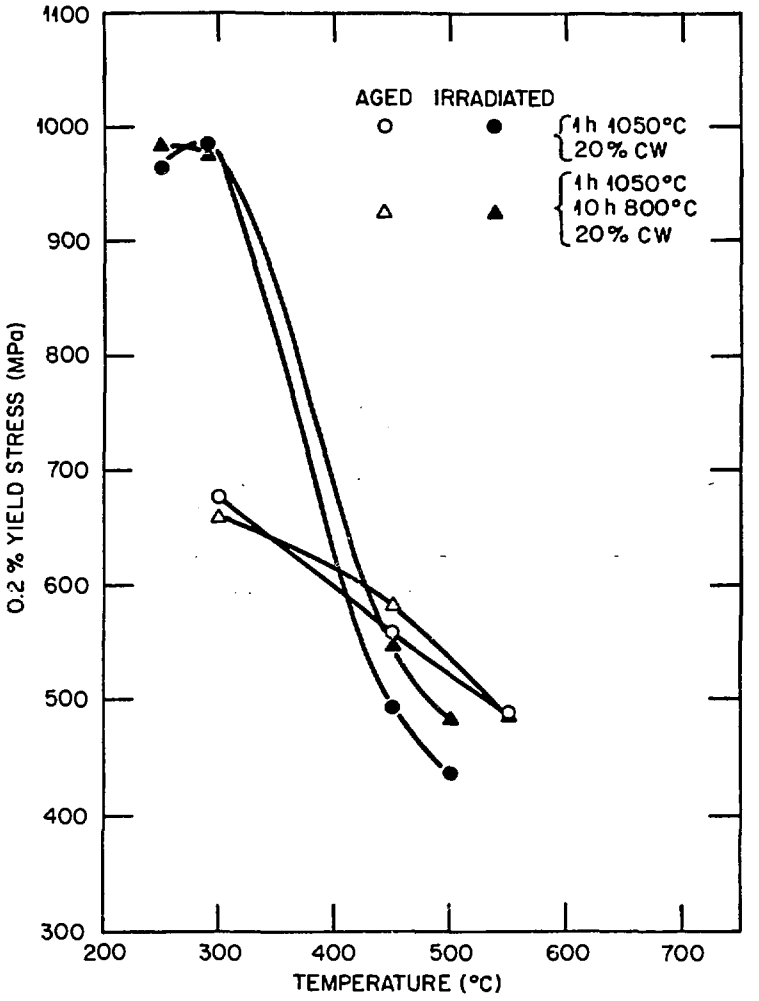

Fig. 9. The 0.2% yield stress of the thermally aged and the irradiated 20%-cold-worked type 316 stainless steel; cold work followed two different heat treatments. Tests were at the aging and irradiation temperatures.

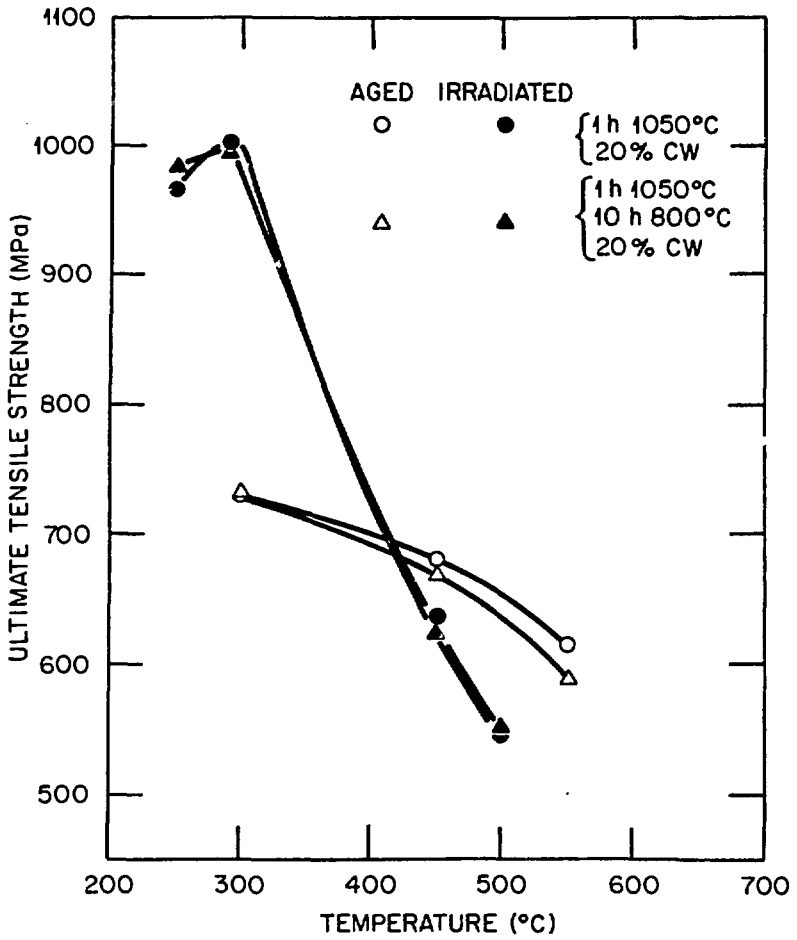

Fig. 10. The ultimate tensile strength of the thermally aged and the irradiated 20%-cold-worked type 316 stainless steel; cold work followed two different heat treatments. Tests were at the aging and irradiation temperatures.

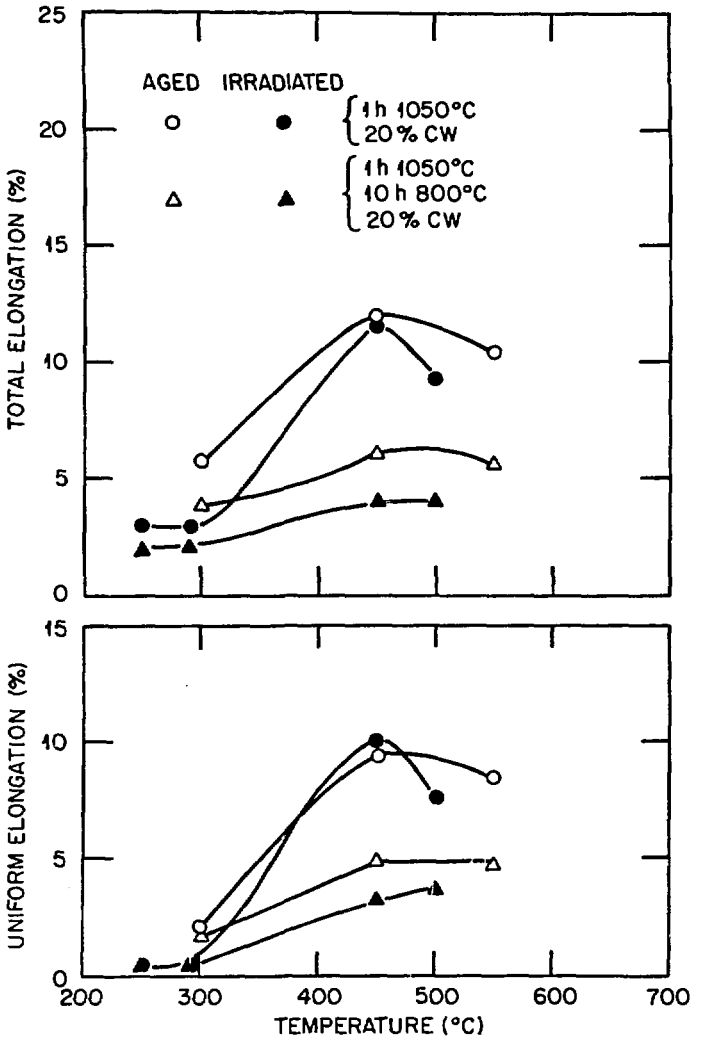

Fig. 11. The uniform and total elongations of the thermally aged and the irradiated 20%-cold-worked type 316 stainless steel; cold work followed two different heat treatments. Tests were at the aging and irradiation temperatures.

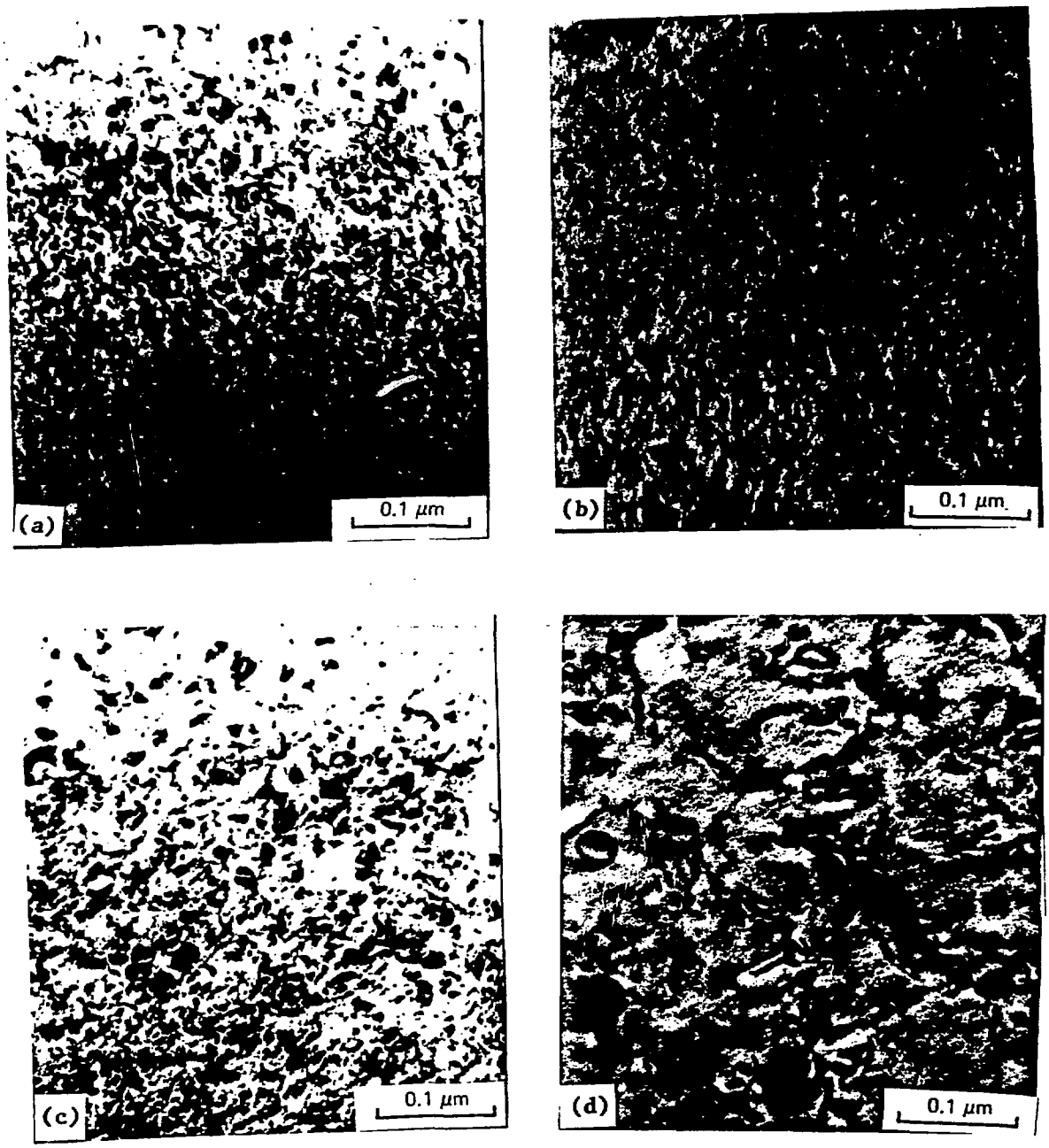

Fig. 12. Dislocation microstructures of CW 316 (reference heat) irradiated in ORR to 5 dpa (38.7 at. ppm He) at (a) 250°C, (b) 290°C, (c) 450°C, and (d) 500°C. All are imaged using g_{200} with $s > 0$. Note the more relaxed structure at 500°C (d).

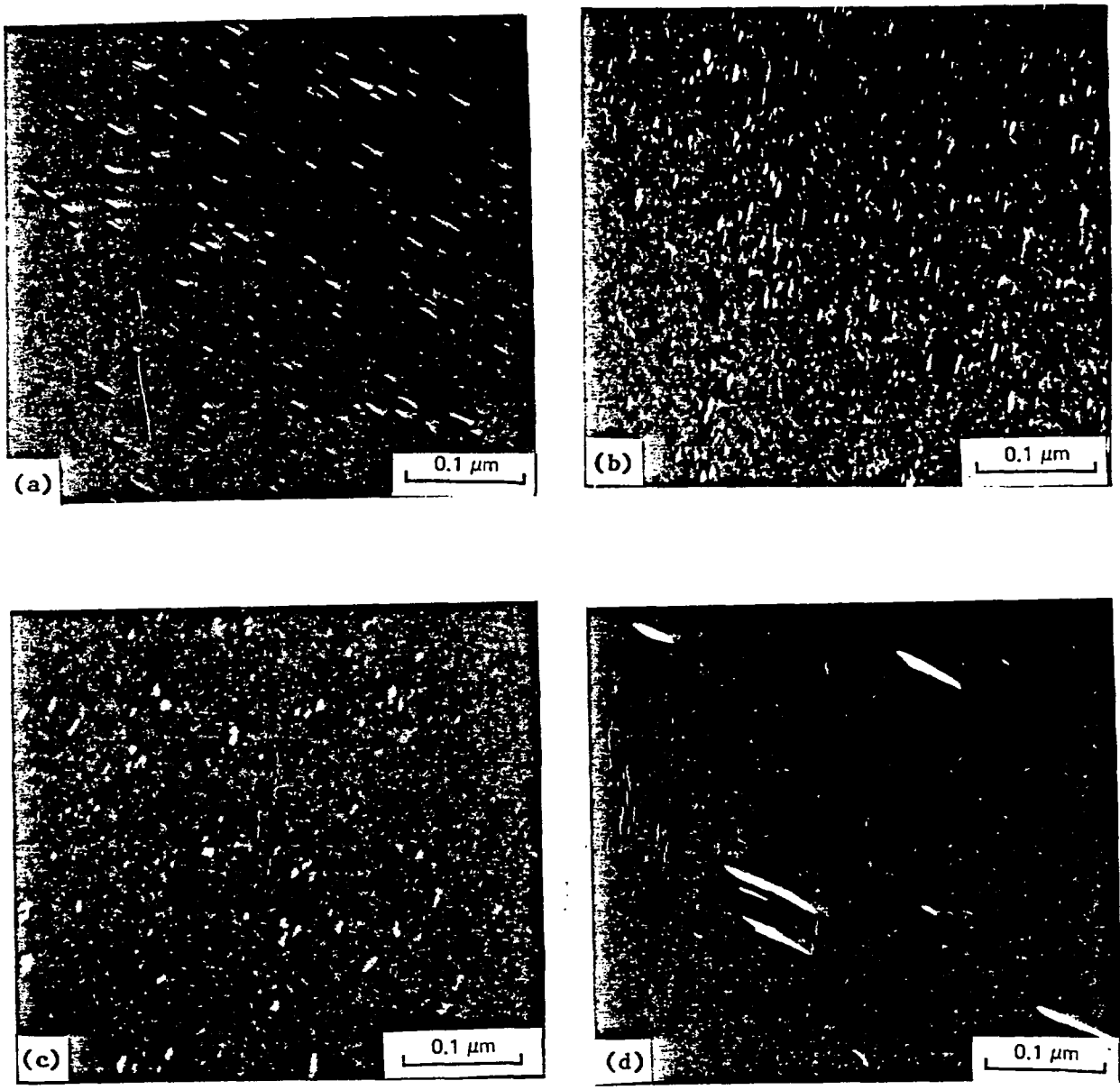

Fig. 13. Larger Frank loop component of the dislocation microstructure of CW 316 (reference heat) irradiated in ORR to 5 dpa (38.7 at. ppm He) at (a) 250°C, (b) 290°C, (c) 450°C, and (d) 500°C. All are imaged in dark field using <111> satellite streaks around g_{200} reflections. Note the large increase in size and decreased density of loops at 500°C, compared with the three lower temperatures.

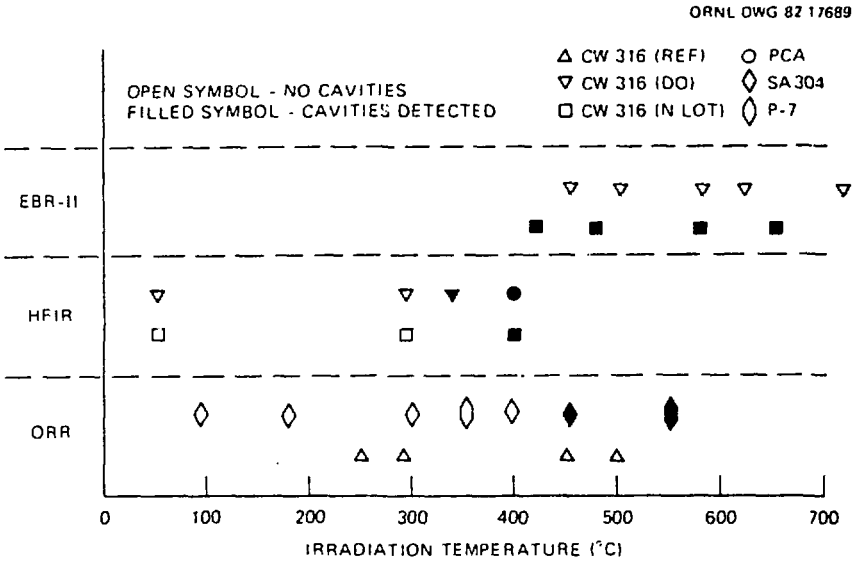

Fig. 14. Temperature boundaries between the various components of the dislocation microstructure observed in austenitic stainless steels irradiated to fluences producing 12 dpa or lower.

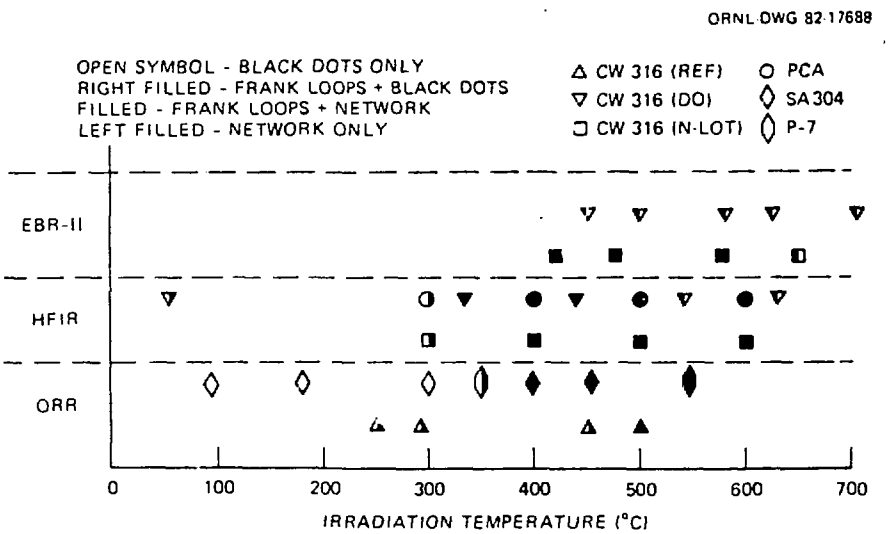

Fig. 15. Observations at fluences producing 12 dpa or lower that define the lower temperature limit for cavity formation in austenitic stainless steel.